*Journal of Computational Design and Engineering*, 2023, **10**, 1126–1142
DOI: 10.1093/jcde/qwad041
Advance access publication date: 11 May 2023
Research Article

# Virtual reality-based assembly-level design for additive manufacturing decision framework involving human aspects of design

Ulanbek Auyeskhan[1,2,†], Clint Alex Steed[1,3,†], Soohyung Park[1], Dong-Hyun Kim[2], Im Doo Jung[1] and Namhun Kim[1,*]

[1]Department of Mechanical Engineering, Ulsan National Institute of Science and Technology, Ulsan 44919, Republic of Korea
[2]3D Printing Manufacturing Process Center, Korea Institute of Industrial Technology, Ulsan 44776, Republic of Korea
[3]Department of Industrial Engineering, Stellenbosch University, Stellenbosch 7600, South Africa
*Corresponding author. E-mail: nhkim@unist.ac.kr
†Equal contribution

## Abstract

There is a combinatorial explosion of alternative variants of an assembly design owing to the design freedom provided by additive manufacturing (AM). In this regard, a novel virtual reality-based decision-support framework is presented herein for extracting the superior assembly design to be fabricated by AM route. It specifically addresses the intersection between human assembly and AM hence combining design for assembly, and design for additive manufacturing using axiomatic design theory. Several virtual reality experiments were carried out to achieve this with human subjects assembling parts. At first, a two-dimensional table is assembled, and the data are used to confirm the independence of non-functional requirements such as assembly time and assembly displacement error according to independence axiom. Then this approach is demonstrated on an industrial lifeboat hook with three assembly design variations. The data from these experiments are utilized to evaluate the possible combinations of the assembly in terms of probability density based on the information axiom. The technique effectively identifies the assembly design most likely to fulfill the non-functional requirements. To the authors' best knowledge, this is the first study that numerically extracts the human aspect of design at an early design stage in the decision process and considers the selection of the superior assembly design in a detailed design stage. Finally, this process is automated using a graphical user interface, which embraces the practicality of the currently integrated framework and enables manufacturers to choose the best assembly design.

**Keywords:** axiomatic design, decision making, design for additive manufacturing, design for assembly, part consolidation, digital twin

## 1. Introduction

Before three-dimensional (3D) printing of an assembly, specifically at the early design stages, one should be able to identify which assembly design is the best among many alternatives provided by part consolidation (PC). PC is the opportunistic facet of design for additive manufacturing (DfAM) that allows combining parts resulting in a reduced part count of an assembly (Biswal *et al.*, 2020). Various techniques are available that address PC both conceptually (Sossou *et al.*, 2018; Yang & Zhao, 2016) and numerically (Kim & Moon, 2020; Nie *et al.*, 2020). For example, a study by Yang *et al.* (2018) provides a numerical approach for how to select part candidates for 3D printing particular assemblies. Another study by Schmelzle *et al.* (2015) shows a conceptually design-case-oriented PC that resulted in a single component printed by using laser powder bed fusion enabling better performance.

Moreover, at the early design stage, a customer with a multi-component assembly would want to have the most desired assembly based on human aspects of design. The reason is that human aspects of design capture a direct interaction of human subjects with design artifacts (Maier & Fadel, 2009). In this context, design artifacts are the parts of assemblies aimed to be fabricated via additive manufacturing (AM) route. Two important questions arise from this: Firstly, how can human-centered design aspects be effectively integrated? Secondly, how can both conceptual and theoretical approaches be incorporated to select the optimal assembly design? Therefore, for the first question, virtual reality (VR) is reported to be the most relevant tool for human involvement in the experiment (Abidi *et al.*, 2019; Brookes *et al.*, 2020). To aid in the selection of the best assembly design, axiomatic design (AD) theory is one of the design methodologies that could be employed (Suh, 1995).

The present study will focus on VR and AD applications to involve human aspects in selecting the best assembly DfAM. The study by Abidi *et al.* reveals that the participants who received VR training demonstrated a higher level of performance, as evidenced by a reduction in the number of errors and a decrease in the time required to assemble the actual product when compared with those in the traditional or baseline training group (Abidi *et al.*, 2019). In the case of AD, it has been extensively utilized for almost three decades in different sectors: software (Harutunian *et al.*, 1996), manufacturing systems (Rauch *et al.*, 2016), decision-making (Wang *et al.*, 2020), and other sectors (Kulak *et al.*, 2010). AD was used herein to lay a scientific foundation with its two

**Received:** December 24, 2022. **Revised:** April 25, 2023. **Accepted:** April 26, 2023

developed axioms (Suh & Sekimoto, 1990): independence (AD-1) and information axioms (AD-2). According to AD-1, a provision of independence must be supplied between functional requirements (FRs) and the design parameters (DPs) inherited by design. AD-2 can be referred to as a selection filter for designs that already satisfy AD-1.

AD has been utilized as a basis for the design framework for AM in the study by Renjith *et al.* (2020). That AM framework was created through a rigorous process of identifying and defining the design problem based on FRs, DPs, and the capabilities of AM. By systematically considering these factors, the framework provides a structured approach to designing for AM, helping to ensure that the resulting product is optimized.

The work by Agrawal showcases the usage of AD by incorporating AM experts' opinions on their design guideline's importance which also includes PC (Agrawal, 2022). By assigning grey numbers for category ranking, they could identify which AM capabilities are more important based on a conducted survey at the early design stages.

Although AD has been used in the early design phases, there exist several limitations in AM design frameworks in which AD was utilized, as listed below:

(i) The absence of a VR experimental approach for constructing and verifying a design matrix for the independence of FRs within a functional domain.
(ii) Another issue that has been reported is that the human aspects of design are often overlooked during the early stages of design development. This involves not only seeking expert opinions but also examining the effects of human subjects' interactions with a design artifact on either part or assembly design.

Furthermore, when dealing with many parts, there are numerous possible combinations of PC for an assembly design. This can make it challenging to determine the most optimal way to design an assembly for AM. Some studies have focused on finding candidates for PC (Kim & Moon, 2020; Yang *et al.*, 2019). Indeed, designers and engineers can sort out their desired assembly based on their experience; however, in this digital era, theoretical and practical bases are required to filter the potential assembly design intended for AM. In addition, regarding the manufacturability of products, assemblability should be considered or, in other words, design for assembly (DfA) to satisfy customer requirements. To demonstrate this, VR experiments were conducted on various alternatives of 2D tables to verify the independence of non-functional requirements (nFRs) such as assembly time and assembly displacement error. Furthermore, a case study on industrial lifeboat hook assemblies involving human subjects in VR environments is also provided to showcase the framework's applicability.

To achieve the points mentioned above, a comprehensive decision framework is necessary, as shown in Fig. 1, which provides a brief overview. The primary purpose of this framework is to select the best assembly design among many possible consolidated alternatives. For this, following Fig. 1, first, customer needs (CNs) are dictated by stakeholders and mapped to respective requirements. Along with these requirements, DfAM-specific constraints are applied to narrow down the number of possible assembly designs. Then the design matrix which includes a correlation between the requirements should be verified for independence by VR experiments as per AD-1. If that satisfies, one can go for the next stage of selecting the best assembly design based on the design matrix.

Following that, data processing should be performed resulted by digital twins in the form of a virtual prototype of an actual assembly system to ensure applicability in AD-2. Finally, an assembly design can be achieved that most likely satisfies the design range (DR) in terms of probability density.

To emphasize, the novelties of this study are: (i) human involvement through assembly time and assembly displacement error that occur during the assembly process under DfAM constraints and (ii) filtering the best assembly design but not finding the best part candidates for PC.

The following is how this paper is organized: Section 2 provides background for AD and its applications in AM and DfAM. Section 3 presents the newly proposed DfAM decision framework. Section 4 details the experimental design used to extract the human aspect of design and verify AD-1 with a pre-established design matrix involving human subjects. In Section 5, a case study of a lifeboat hook assembly is presented to demonstrate the decision-making framework. Finally, the results are reported in Section 6 along with a discussion of selecting an assembly that is superior to others.

## 2. Literature Review

Numerous approaches to the early design stage have been proposed, including, DfAM-based guidelines (Pradel *et al.*, 2018), inverse problem solving (Rodrigue & Rivette, 2010), TRIZ (Renjith *et al.*, 2018), AD (Salonitis, 2016), machine learning-integrated DfAM (Jiang *et al.*, 2022), and the integration of these methods (Tamayo *et al.*, 2019; Zhang *et al.*, 2007). Among these aforementioned methods, AD has gained significant attention owing to its ability to provide structured and systematic design solutions. It was developed by Suh and Sekimoto in 1990 (Suh & Sekimoto, 1990) as a theoretical framework to promote a more effective design approach. According to Lee and Suh (2006), the design world comprises four primary domains: customer domain, functional domain, physical domain, and process domain. The interaction among these domains can be interpreted as "what a customer needs" and "how this need can be satisfied." The notion of domains is interconnected by dividing lines between the four types of design activities. Further, it is a fundamental cornerstone of AD that facilitates the standardization of the thinking process involved in this interplay.

Specifically, the needs, attributes, or traits that a customer is seeking in a particular product define the "customer domain". Then, within a set of "FRs" and "constraints", the CNs are mapped to the "functional domain". The DPs in the "physical domain" are created to fulfill the FRs and constraints specified. Finally, in the "process domain", processes that should satisfy FRs are defined using "process variables" (PVs).

The mapping process between the domains facilitates decisions on an appropriate design solution. These decisions assume that they will not contradict two governing axioms of AD. Examining the common aspects that are always included in successful designs yielded these abovementioned axioms: (i) AD-1 and (ii) AD-2 (Suh, 1995).

### 2.1. Independence axiom (AD-1)

AD-1 is the AD's core axiom which states that FRs should be independent of each other. However, FRs' independence, does not always imply physical independence; thus, the two should not be confused with each other (Green *et al.*, 2022).

As mentioned previously, because AD can offer a theoretical foundation, the mapping process can be described mathematically. For example, the domain vectors {FR} and {DP} can be related

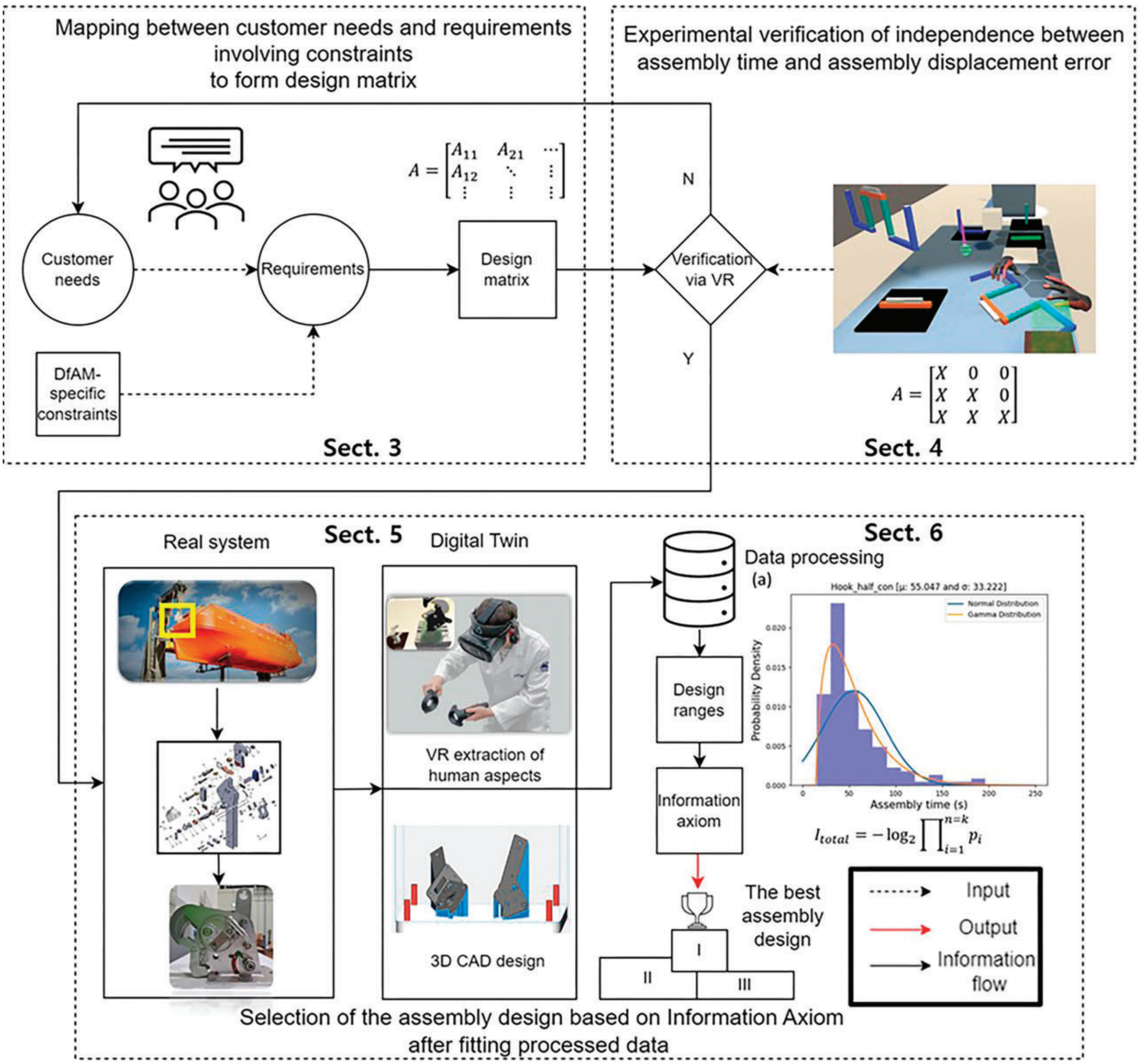


**Figure 1:** Overview of the proposed decision framework. A real system refers to a case study. Input, output, and information flows are indicated accordingly.

by the design matrix, $[A]$. This is shown in Equation (1) as

$$\{FR\} = [A]\ \{DP\}. \tag{1}$$

The design matrix, $[A]$ should either be a diagonal or a triangular matrix to refrain from violating AD-1. Examples of diagonal and triangular matrices are shown below:

$$\begin{bmatrix} FR1 \\ FR2 \end{bmatrix} = \begin{bmatrix} A_{11} & 0 \\ 0 & A_{22} \end{bmatrix} \begin{bmatrix} DP1 \\ DP2 \end{bmatrix} \tag{2}$$

$$\begin{bmatrix} FR1 \\ FR2 \end{bmatrix} = \begin{bmatrix} A_{11} & A_{21} \\ 0 & A_{22} \end{bmatrix} \begin{bmatrix} DP1 \\ DP2 \end{bmatrix}. \tag{3}$$

The diagonal matrix is called uncoupled, as shown in Equation (2), whereas the design matrix presented in Equation (3), an upper triangular matrix (or a lower triangular matrix), is called a decoupled design matrix.

Similarly, in terms of design matrices, these relationships between {DP} and {PV} should also be maintained. The design matrices are not expressed numerically in the described equations. At the early conceptual design stage, numerical values in the design matrices need not explain the extent of independence because knowing they are independent is sufficient (Farid & Suh, 2016).

Re-angularity and semi-angularity have been reported to numerically express the design matrix that could have been employed when a sufficient set of data is available in advance (Sozo & Forcellini, 2003). Furthermore, there are instances in which AD-1 could not provide a final solution among alternative designs by applying re-angularity and semi-angularity; as a result, AD-2 was applied to obtain the desired outcome (Delaš *et al.*, 2018).

The FRs and DPs (as well as PVs) must be decomposed into a hierarchical relation between the domains until we attain a complete comprehensive design. Therefore, this must organize large systems or assembly components. This process is called the zigzagging decomposition approach, which leads a designer to

**Table 1:** Summary of studies that utilized AD for AM in terms of opportunistic and restrictive DfAM, verification of AD-1 via VR, and inclusion of human aspects of design.

| AD works in DfAM | Opportunistic | Restrictive | Verification of AD-1 | Human aspects of design |
|---|---|---|---|---|
| Salonitis (2016) | x | o | x | x |
| Renjith *et al.* (2020) | o | o | x | x |
| Toguem *et al.* (2020) | x | o | x | x |
| Chekurov *et al.* (2019) | o | o | x | x |
| Boca *et al.* (2021) | x | o | x | x |
| Agrawal (2022) | o | o | x | x |
| This study | o | o | o | o |

observe the final subproblem/subtask/subassembly. In particular, a mapping is performed in the domain from the left to the right domain at the highest level and then reversed to the lower level of the left domain (Lee & Suh, 2006). The mapping will be discussed in detail in Section 3.

Furthermore, several designs may be acceptable by AD-1 because of the decomposition of a particular product. Among the qualified designs, one can outperform others; hence AD-2 is applied.

## 2.2. Information axiom (AD-2)

AD-2 can quantitatively define the best design that satisfies AD-1 in terms of information content $I_{total}$ given by Equation (4) (Chekurov *et al.*, 2019; Chen *et al.*, 2015). The selected design should have the minimum $I_{total}$ implying that, compared with other alternatives, it does not require much information to construct the given design. $I_{total}$ is measured in terms of the probability of success $p_i$; hence it has a negative sign:

$$I_{total} = -\log_2 \prod_{i=1}^{n=k} p_i \quad (4)$$

where $I_{total} = [0, +\infty)$.

## 2.3. Applications of AD in AM and DfAM

The applications of AD were comprehensively described in literature reviews published between 1990 and 2009 (Kulak *et al.*, 2010) as well as 2013 and 2018 (Heikkilä, 2020). The first mention of AM in AD was in terms of rapid prototyping (Suh, 2001). Furthermore, an iterative improvement of the test part features designed to evaluate 3D printing processes at the microscale using AD was also reported (Thompson & Mischkot, 2015). Others have used both axioms of AD to select the most appropriate 3D printing technology for specific applications (Gangwar *et al.*, 2009). Furthermore, in the context of DfAM, Salonitis (2016) has proposed a guide on how AD principles can be used as a foundation for developing DfAM strategies. He used a bracket to validate the framework by setting high-level FRs, DPs, and PVs. Another work by Agrawal (2022) identified the most critical 26 DfAM and design for environment guidelines as FRs to be applied in AD, relying on both literature surveys and experts' opinions. In addition, they also categorized all the guidelines into five groups using AD. Toguem *et al.* have proposed an AM design approach based on AD. The design artifact was manufactured via the laser powder bed fusion (L-PBF) platform and subsequently evaluated according to pre-defined Geometric Dimensioning and Tolerancing (GD&T) features. AD was also applied in aiding designers to understand the increased design freedom and limitations of AM (Chekurov *et al.*, 2019). A case study of non-assembly turbine design shows that AD can be used to design parts with better performance, affordable cost, and reduced information content while considering restrictive facets of DfAM, such as minimum wall thickness and maximum size of parts. Another study showed that the application of AD in AM resulted in an optimized design of molds or tools that could be utilized for conventional manufacturing processes (Boca *et al.*, 2021). Allowing for quicker production with a high degree of flexibility in design, the study found that their method offers prevalence in production cost and time. A study conducted by Renjith *et al.* (2020) integrated AD and TRIZ to form a DfAM framework. Even though the authors do not involve AD-2, an original link-pin assembly was redesigned to improve dependability and reduce weight.

Nevertheless, while some authors have utilized opportunistic and/or restrictive DfAM, there is a scarcity of evidence demonstrating that the use of AD-1 within DfAM frameworks to create a design matrix through VR and to numerically capture human aspects related to the interaction between human subjects and design artifacts as shown in Table 1. In particular, the studies by Maier and Fadel (2009) and Green *et al.* (2022) have reported that, apart from subjective opinions gathered during the initial stages of design, the human aspects of design, such as the thought processes of individuals, interactions during the design phase, engagement with objects, and other key design elements, are not captured in AD. In this study, human aspects of design primarily refer to the interaction of human subjects with design artifacts.

Furthermore, in an assembly that will be 3D printed using PC approaches, one can have multiple alternative variants owing to the possibility of functional integration of assembly components and enhanced performance (Nie *et al.*, 2020). Thus, filtering the best design among these combinations by considering constraints of the functional domain and an inclusion of human aspects of design in AD within DfAM frameworks has not yet been investigated.

To address the aforementioned issues, a new assembly-level design framework involving DfAM-specific constraints and human aspects based on AD was proposed. Furthermore, the framework enables the production of assembly parts through a compatible AM process, such as metal L-PBF. Additionally, not all practitioners demonstrate AD-2 in DfAM, even though it is critical when many alternative designs are available. Finally, an in-house graphical user interface (GUI) is introduced to enhance the practicality of the proposed framework.

# 3. Novel DfAM Decision Framework Based on AD

In this section, we explain how the AD-adopted DfAM decision framework was developed with a focus on the inclusion of human assembly processes. The previous lack of human aspects of design in AD-based DfAM frameworks will be addressed by offering experimental design factors and

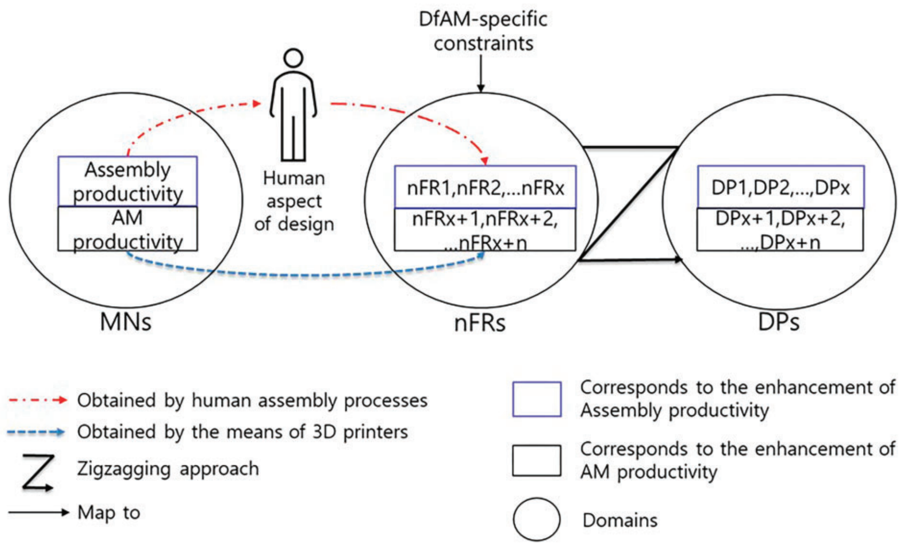


**Figure 2:** Enhancement of assembly and AM productivities via human involvement mapped to non-FRs. PVs are not shown here as process parameters are assumed to be fixed.

data-driven distributions. Before that, domain-specific definitions are
clarified.

In practice, many stakeholders provide design requirements in product design phases. One such requirement is from the perspective of the end-users, wherein FRs are considered as the primary factor, while the second requirement is from the perspective of the assembly or manufacturing process, which conveys information through so-called nFRs (Thompson, 2013). Thompson was the first to mention nFRs, emphasizing that they should be explicitly identified to comply with a manufacturing point of view. In this regard, our new approach constitutes the extraction of nFRs instead of FRs; however, mathematically, FRs and nFRs serve a similar role in both axioms. Furthermore, they can be regarded within the same functional or requirement domain, as reported by (Mabrok *et al.*, 2015). Characterizing key CNs during the design process ensures that no significant components of the problem are overlooked. Herein, CNs are referred to as manufacturing process needs (MNs), as mentioned by Oh and Behdad (2017). Nevertheless, for the selection of assemblies, we assume that FRs are already satisfied; hence the main emphasis is on nFRs.

## 3.1. Human involvement in the design process: assembly time and assembly displacement error

In this study, nFRs were extracted from MNs to enhance assembly and AM productivity separately, unlike in Oh and Behdad's work. The number of parts and fasteners, handling, and insertion issues are considered in terms of DfA to evaluate assembly complexity (Boothroyd & Alting, 1992). Furthermore, there are both manual and automatic assembly types (Mattsson, 2013). This study focuses on manual assembly to both enhance assembly productivity in low-volume manufacturing and to demonstrate the human aspect of assembly designs.

In the first stage of the proposed approach, as shown in Fig. 2, to improve DfA productivity, assembly time (nFR1) and assembly displacement error (nFR2) should be verified for their independence. Additionally, the support volume (nFR3) of different assembly designs of a real case study under DfAM constraints is considered to enhance AM productivity. After the identification of nFRs, DPs are also obtained, as demonstrated in the coming sections. Next, the motivation behind providing the abovementioned nFRs is explained in brief.

nFR1 – assembly time: It is a critical factor in supply chain that governs a major portion of the manufacturing costs. Reducing assembly time of a product by 50%–75% via the implementation of the DfA rules results in a financial gain for industry sectors (Boothroyd & Marinescu, 2008).

nFR2 – assembly displacement error: It is a crucial metric for evaluating different combinations of PC assemblies. In this study, this is used

(i) to assess the design complexity qualitatively;
(ii) to quantify assembling error during manual assembly;
(iii) to offer an assembly line worker a controlled environment; and
(iv) to offer ways of interaction between people and the assemblies before the launch of the product to accelerate the learning process of assembling.

nFR3 – support volume: Before 3D printing, build orientations of the parts in the assembly must be properly managed. Owing to the large projected area, the support volume increases as the number of parts consolidated increases (Nie *et al.*, 2020). This subsequently renders the removal of the support parts even more difficult (Auyeskhan *et al.*, 2021).

To reiterate, nFR1 and nFR2 directly pertain to the human aspect of assembly designs because, in DfA, humans are extensively involved within manual assembly (see Fig. 2).

However, it should be demonstrated that nFRs are in the same highest level hierarchy before determining their DRs. This issue is associated with the construction and verification of the design matrix, which is primarily overlooked. For example, one may regard that as nFR1 increases, nFR2 reduces, implying that they are dependent and mutually inclusive. However, this may not necessarily be true. To avoid this, an experiment comprising four different 2D tables was performed to validate independencies in the first place. The details are presented in Section 3.3.2. Before, the

**Table 2:** Correlation matrix generated between a pair of nFRs.

| Corr | nFR1 | nFR2 | … | nFRk | … |
|---|---|---|---|---|---|
| nFR1 | 1 | $r_{12}$ | | $r_{1k}$ | |
| nFR2 | | 1 | | $r_{2k}$ | |
| … | | | | | |
| nFRj | | | | $r_{jk}$ | |
| … | | | | | |

DfAM-specific constraints must be clarified within the decision framework.

## 3.2. DfAM-specific constraints and study assumptions

In this study, nFRs are included within the functional domain, and along with the nFRs, some constraints limit the acceptable designs. However, constraints, unlike nFRs, are not expected to be independent; thus, it is not necessary to prove their mutual independence (Weber *et al.*, 2015).

Herein, the primary constraint is keeping the build time and build cost of the assemblies constant, as our focus is to address human aspects among the assembly alternatives. The assumption is valid because as the number of consolidated parts increases, the support volume also increases, increasing the cost of assembly, as mentioned previously by Nie *et al.* (2020). However, if there are many unconsolidated parts, the cost associated with assembly time will be substantially higher, particularly in the metal L-PBF system. Therefore, based on the two mentioned scenarios, the outcome of build time and cost are assumed to be identical. Moreover, these constraints are directly affected by the build orientations of the parts of assemblies; thus, build orientations are controlled in a manner in which the parts have a minimum volume of support structures. Furthermore, post-processing must be considered to enable the removability of supports. Additionally, when it is necessary to join the parts in an assembly, welding costs also become a concern; nevertheless, in this study, we assume that they are considerably lower than the 3D printing cost; thus they are neglected (Chayoukhi *et al.*, 2009). Regarding the nFR2, the assumption was made that insertion parts such as bolts with nuts were not considered as they do not result in any assembly displacement errors to demonstrate the assembler's interaction with a specific design.

## 3.3. Verification of independence between assembly time and assembly displacement error

### 3.3.1. *Correlation matrix*

As previously stated, before constructing the design matrix, it is required to verify that a pair of nFRs are orthogonal. This can be proven by a correlation matrix (Asuero *et al.*, 2006) via using Table 2. For example, if there is a need to confirm the independence between nFRj and nFRk, a correlation coefficient will be represented as in Equation (5). Thus, it will be utilized to verify the independence of assembly time and assembly displacement error via VR settings as illustrated in Section 4.4.

$$Corr\ (nFRj,\ nFRk) = \frac{\sum_i^N \left(nFRj_i - \mu_{nFRj}\right)\left(nFRk_i - \mu_{nFRk}\right)}{\sqrt{\sum_i^N \left(nFRj_i - \mu_{nFRj}\right)^2}\sqrt{\sum_i^N \left(nFRk_i - \mu_{nFRk}\right)^2}} = r_{jk} \quad (5)$$

here $-1 \le r \le 1$;

$r_{jk}$ – correlation coefficient
$\mu$– mean of respective nFRs; and
$i$– element of nFRs.

### 3.3.2. *Decomposition of nFRs-DP*

The next step is to identify the associated DPs. Here, the zigzagging method can be used to map between nFRs and DPs (Suh, 2001), as shown in Fig. 3. Corresponding DPs are assembly alternatives (DP1), the number of edges and connectors (DP2), and build orientation (DP3). DP1 and DP2 can be further decomposed. Each DP is described in detail in Section 4.4. In the case of PVs, as process parameters are primarily fixed in industrial 3D printers, it is a valid assumption that all DPs could be obtained using already optimized process parameters with respective pre- and post-processing of a build print. Thus, it is assumed that the design matrix obtained from the DP–PV relationship also follows AD-1.

## 3.4. Data acquisition to select the superior design

One of the insights of this work is the acquisition of data from digital prototypes. Specifically, the assembly time and assembly displacement error (human assembly data) were gathered from a VR simulation and support volume (manufacturing) data from third-party software.

Primarily, digital twins have been utilized for various tasks in the literature, including optimization, security improvement, monitoring, predicting, user training, and enhancing a physical prototype or a process (Liu *et al.*, 2022; Segovia & Garcia-Alfaro, 2022). Through VR technology, it is possible to interact between a virtual and real environment. For instance, data can be gathered from digital twins using VR's controllers, as shown in Fig. 4d, in a real-time setting. After confirmation of design matrix satisfaction by AD-1, one can proceed to populate digital twin data, which contain human aspects of design via VR experimentations and pre-processed 3D printing assembly design. These data are used in the decision framework to evaluate the best design.

### 3.4.1. *Assembly time (nFR1)*

To determine the assembly time in a VR scene, the starting time and submission time of each assembly were recorded (Fig. 4e). In addition, VR technology was used to create a simulated assembly environment closely resembling real-world conditions. Human subjects were able to accomplish the assembly tasks in a natural and intuitive manner as a result of the utterly immersive assembling experience. Thus, VR allows us to collect information on human subjects' movements and interactions with design artifacts which can help to quantify assembly time and displacement error in assembly procedures.

### 3.4.2. *Assembly displacement error (nFR2)*

The assembly displacement error, sometimes referred to as an error, represents the deviation of the assembled part from its reference position. It is calculated by summing the distances between the reference and actual locations of the parts. The error is calculated using an assembly graph depicted in Fig. 4a–c. The unity module, which is easily reusable, is provided to facilitate this calculation. A brief explanation follows.

The graph's edges capture the distance between actual and reference assembly components, and it is summed to give the error of the assembly at hand. This graph consists of:

(i) **Components** which represent each part of the assembly.

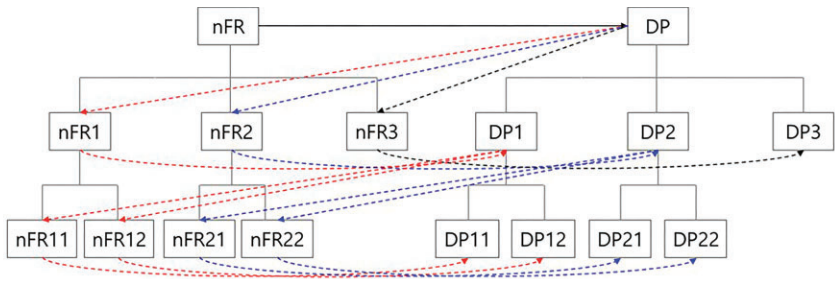


**Figure 3:** Zigzagging method between nFRs and DPs**.** The arrows are used to distinguish the zigzagging approach: red for nFR1, blue for nFR2, and dashed black for nFR3.

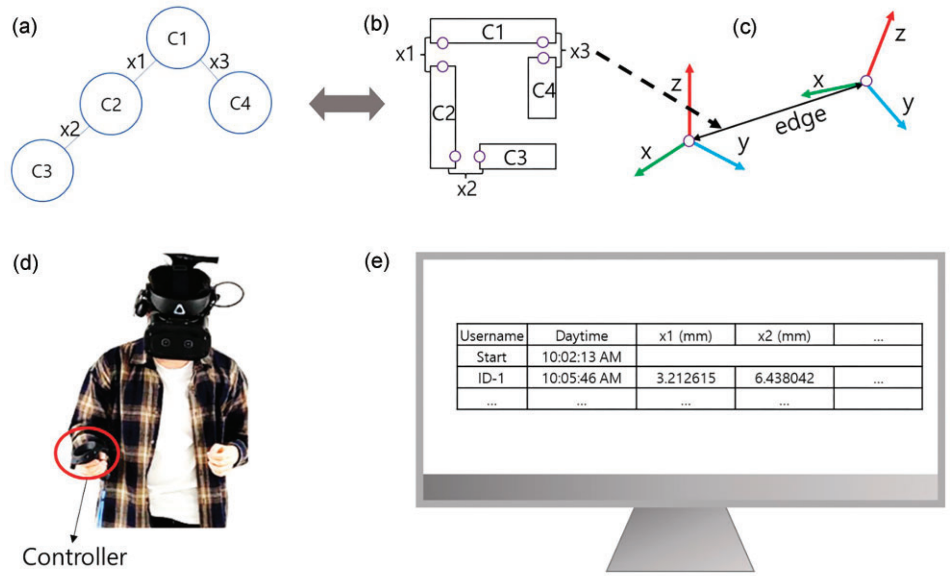


**Figure 4:** (a) Assembly graph example for representative components, (b) representative components with edges and connectors, (c) general representation of the edges in 3D, (d) human subject with VR controller, and (e) assembly time and error recording as soon as connectors are joined.

(ii) Each component has a few **connectors.** These are the points where components fit together. They resemble welding points.

(iii) **Edges** capture the relationship between two connectors. Initially they contain the distances in meter $\Delta x$, $\Delta y$, and $\Delta z$.

(iv) Assembly displacement **error** is calculated by summing the radial distance of each edge as in Equation (6). In this case, L1-norm was used as it places emphasis on the minor errors, where L2-norm would place more weight on larger errors.

$$\text{Error} = \left\| \sqrt{\Delta x^2 + \Delta y^2 + \Delta z^2} \right\|_1 \tag{6}$$

### 3.4.3. *Support volume (nFR3)*

DfAM-specific constraints explained in Section 3.2 should be considered to extract support volume data. The data can be obtained by commercial pre-processing software such as Magics Materialise, for example.

To utilize obtained aforementioned nFRs data in information axiom, data processing needs then be carried out in terms of an appropriate distribution illustrated in Section S1 in the Supplementary file. In addition, DRs are used to define the allowable variations in the design without compromising the nFRs (Oh & Behdad, 2017). Thus, DRs are decided based on the nFRs subjectively because they demonstrate how well the design meets the targets while maintaining its independence.

This section shows how data acquired from digital prototypes were used to compare designs. Both third-party software for the support volume and VR to capture human assembly data were involved. Next, the details of the experimentations will be covered.

# 4. Experiment

## 4.1. Design of experiments

It is worth reiterating that using VR enables the evaluation of the human aspect of design by allowing for interaction with the design beforehand. VR scenes were programmed in such a way that they allow extraction of the activities of human subjects and record the corresponding data (nFR1 and nFR2) in real-time. The process was initiated using simple assemblies from the 2D table and subsequently progressed to utilizing actual assembly parts (see Fig. 5).

## 4.2. Description of assembly operations

Human subjects were expected to assemble the components at the designated areas of each part. They received audio and visual feedback when they finished the task correctly. Initially, human subjects completed a tutorial to familiarize themselves with VR, the process, and the objectives. Then, the primary experimental

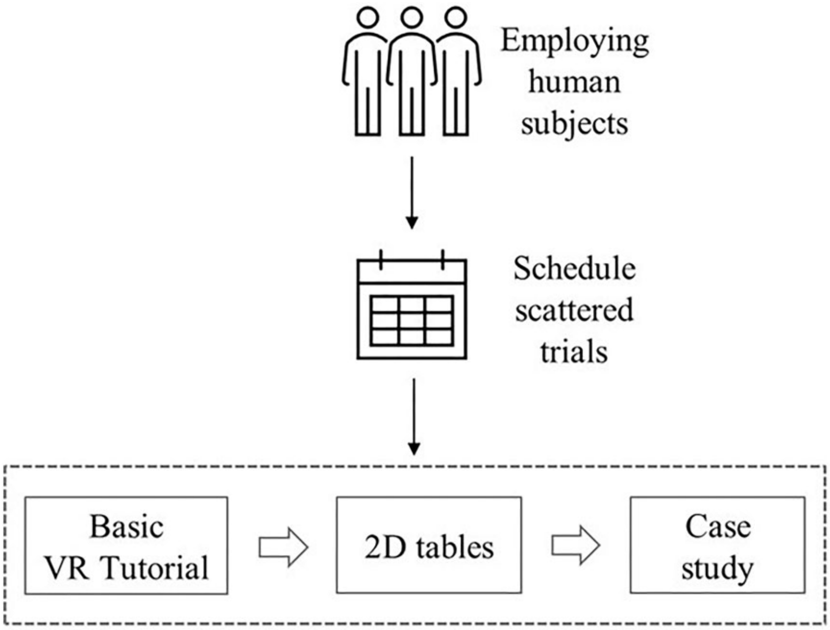


**Figure 5:** Outline of the design of experiments to obtain the human aspect of design (the dashed box represents the set of experiments). Basic VR tutorial and 2D tables are utilized to form the design matrix. Then, one can try to assess target assembly designs. In this study, the authors chose lifeboat hook assemblies described in Section 7.

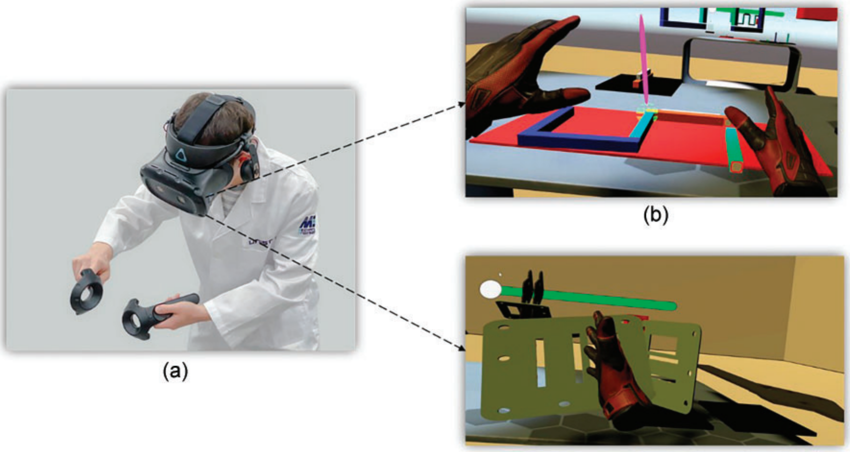


**Figure 6:** (a) Illustration of how a human subject experiments with assembly parts, (b) 2D table scene, and (c) Hook assembly scene.

tasks were conducted several times to facilitate and evaluate the learning process. As it pertains to assembling, the human subjects performed PC by joining the assembly parts.

## 4.3. Experimental procedure

VR experiments with 10 human subjects were conducted to establish this approach. The subjects are all male, with ages ranging from 18 to 29 years. The participants have little to no prior experience with VR. Throughout the 10 days of the experiment (two groups of five participants each performing across 2 weeks × 5 days), all participants tested in the morning and afternoon within non-repeating time slots.

In our study, there are three virtual scenes: (i) tutorial, (ii) 2D tables, and (iii) real assemblies, as shown in Fig. 6. For each assembly task, all participants were shown video instructions and were well compensated for the experiments. In the beginning, all participants passed the tutorial scene and proceeded to the stage with 2D tables. There are four assemblies differing in the number of components, connectors, and edges. Each assembly was tested thrice on the first day, and then it was increased by one each day. The primary reason for the observed efficiency in assembly time is due to Wright learning, in which human subjects start to learn to assemble faster (Wright, 1936). This learning process provides more assembly trials within 5 days. Similarly, in the second scene, the case study of the lifeboat hook was tested, and it followed the same procedure as the scene with the 2D tables.

As mentioned previously, the 2D tables are used to evaluate the orthogonality of nFR1 and nFR2, which pertain to enhancing DfA productivity. Different numbers of components, connectors, and edges are used to establish this independence. For example, as shown in Fig. 7 and Table 3, the pairs of (T1, T3) and (T2, T4) are structurally and functionally the same but have

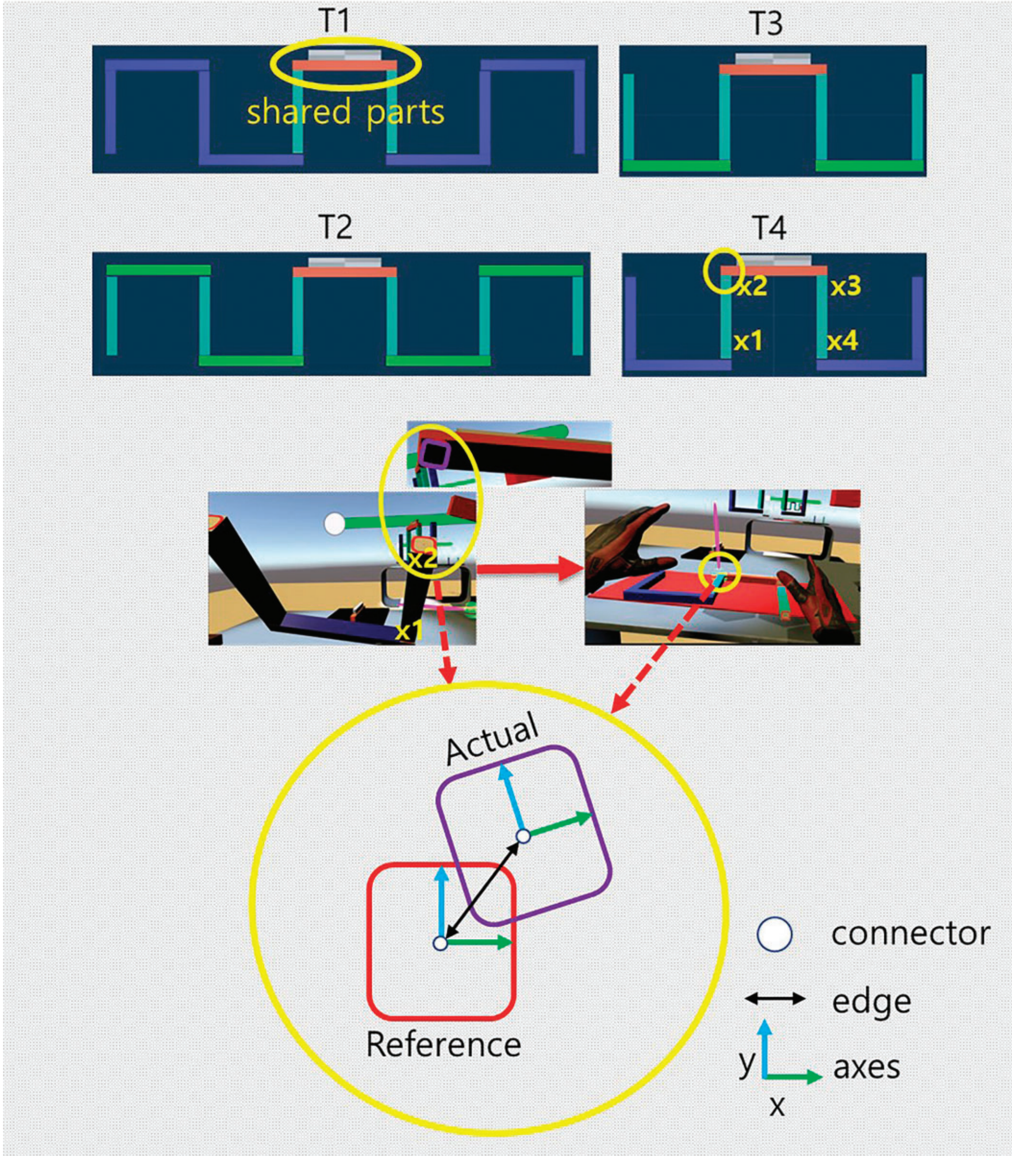


**Figure 7:** 2D tables with different numbers of components. Shared gray and red parts represent the upper side of all 2D tables. The different colored parts are distinguished by the edges. An example of the edges in T4 are highlighted as x1–4. The assembly process is provided as a supplementary video.

different numbers of components. They were intentionally designed to observe the dependence between nFR1 and nFR2. Additionally, these 2D tables and respective numbers of components are chosen to test repeatability and to ensure ease in assembling for the participants. The 2D tables are expected to be assembled on the desk to avoid errors in 3D as if the parts are assembled using jigs and/or holders.

**Table 3:** Number of components, connectors, and edges of the 2D tables.

| 2D table# | Components | Connectors | Edges |
|---|---|---|---|
| T1 | 7 | 14 | 6 |
| T2 | 11 | 22 | 10 |
| T3 | 7 | 14 | 6 |
| T4 | 5 | 10 | 4 |

## 4.4. Verification of independence among nFRs

AD approach consists of several steps to ensure that all MNs are met systematically, as it was pointed out in Section 3.1. The initial step in this study was to obtain a clear understanding of the MNs, with a particular emphasis on improving DfA and DfAM productivities to establish a desired design matrix. Once MNs are determined, the next step is to map them into the functional domain to identify nFRs. These nFRs are then decomposed into lower level nFRs until the lowest level of detail is reached. After analyzing nFRs, DPs, which are the design variables that can be adjusted to achieve the desired nFRs, are identified.

As mentioned earlier, DfA involves part handling and insertion times; thus, nFR1 can be decomposed into part handling time (nFR11) and insertion time (nFR12). The corresponding DPs are the number of parts (DP11) and the number of interfaces (DP12) (see Table 4). nFR11 and DP12 are orthogonal according to Oh and Behdad (2017); hence AD-1 can be satisfied. Orthogonality implies

**Table 4:** Decomposed nFR1.

| nFRs\DPs | | Number of parts DP11 | Number of interfaces DP12 |
|---|---|---|---|
| Less parts handling time (s) | **nFR11** | X | 0 |
| Less parts inserting time (s) | **nFR12** | X | X |

**Table 5:** Decomposed nFR2.

| nFRs\DPs | | Morning or afternoon DP21 | Number of people experimented DP22 |
|---|---|---|---|
| Acceptable fatigue level | **nFR21** | X | 0 |
| Acceptable DFA complexity | **nFR22** | X | X |

direct independence among either FRs or nFRs. In the case of nFR2, it can be further divided into human fatigue level (nFR21) and DfA complexity (nFR22) as well as respective DPs such as daytime (DP21) and the number of human subjects (DP22) (see Table 5). This is explained by the inclusion of the scattered schedule during the experimentation to avoid human fatigue. It is accepted that humans perform better in the mornings (Hines, 2004); hence, these DPs are critical when nFR2 is considered. Additionally, the nFR21 is not related to DP22; thus, this is the lowest level of detail for nFR2.

After a series of experimentations with 2D tables, one can find a correlation between nFR1 and nFR2 as a result of Equation (5). It should be noted that the correlation coefficient was found between each edge of nFR2 and nFR1, also between the L1 norm of nFR2 and nFR1 to observe the independence wholly. Table 6 shows that $\max(|r|) = 0.11742$ implying a very weak correlation (refer to Section S2 of Supplementary file) which can represent the independence of L1 norms of nFR1 and nFR2.

Meanwhile, as DfA and DfAM productivities were distinguished, nFR3 can now be appended to the design matrix without intervening independence of nFR1 and nFR2. Thus, this design matrix will facilitate the consideration of any assemblies for AM, as shown in Table 7. Note that the other key issues which should be concerned in enhancing AM productivity, such as nesting/packing, pre- and post-processing as well as material preparation, are already assumed to be considered within DP–PV relation as mentioned in Section 3.4.

nFR1 and nFR2 include both the design aspect of the artifacts and human aspect of the design. The rationale is that every artifact has different nFR1 and nFR2 from a design perspective. Finally, the systematic and experimental approach to construct and verify a design matrix results in a decoupled design, as described in Equation (7). It should be clarified that after the verification of independence of nFRs in the early design stages, a detailed design stage is of a concern to finally select the best assembly design.

$$A = \begin{bmatrix} A_{11} & A_{21} & A_{31} \\ A_{12} & A_{22} & A_{32} \\ A_{13} & A_{23} & A_{33} \end{bmatrix} = \begin{bmatrix} X & 0 & 0 \\ X & X & 0 \\ X & X & X \end{bmatrix} \tag{7}$$

## 5. Case Study – Lifeboat Hook Assembly

The proposed decision framework is illustrated by involving the Hyundai lifeboat hook assembly from the previous

**Table 6:** Correlation matrix between nFR1 and nFR2. Labels x1–x10 represent the edges. L1-norm of nFR2 versus nFR1 shows very weak correlation (|r|<0.199) hence there is an independence between them.

| 2D tables | | Assembly displacement errors (nFR2) | | | | | | | | | | L1-norm of nFR2 versus nFR1 |
|---|---|---|---|---|---|---|---|---|---|---|---|---|
| | | x1 | x2 | x3 | x4 | x5 | x6 | x7 | x8 | x9 | x10 | |
| Assembly time (nFR1) | T-1 | −0.191 86 | −0.120 51 | 0.134 008 | −0.131 45 | −0.061 56 | −0.219 13 | | | | | −0.113 49 |
| | T-2 | −0.101 72 | −0.143 96 | −0.159 53 | −0.0797 | −0.016 67 | −0.004 49 | 0.010 255 | 0.008 542 | 0.061 481 | −0.067 47 | −0.042 91 |
| | T-3 | −0.149 49 | −0.106 66 | −0.2235 | −0.075 58 | −0.034 | 0.014 856 | | | | | **−0.117 42** |
| | T-4 | −0.0957 | −0.137 59 | −0.075 52 | −0.0398 | | | | | | | −0.109 76 |

**Table 7:** Design matrix to enhance DfA and DfAM productivities.

| nFRs\DPs | | Assembly alternatives DP1 | Number of edges and connectors DP2 | Build orientation DP3 |
|---|---|---|---|---|
| Less assembly time (s) | **nFR1** | A11 | A21 | A31 |
| Assembly displacement accuracy error (mm) | **nFR2** | A12 | A22 | A32 |
| Support volume range ($cm^3$) | **nFR3** | A13 | A23 | A33 |

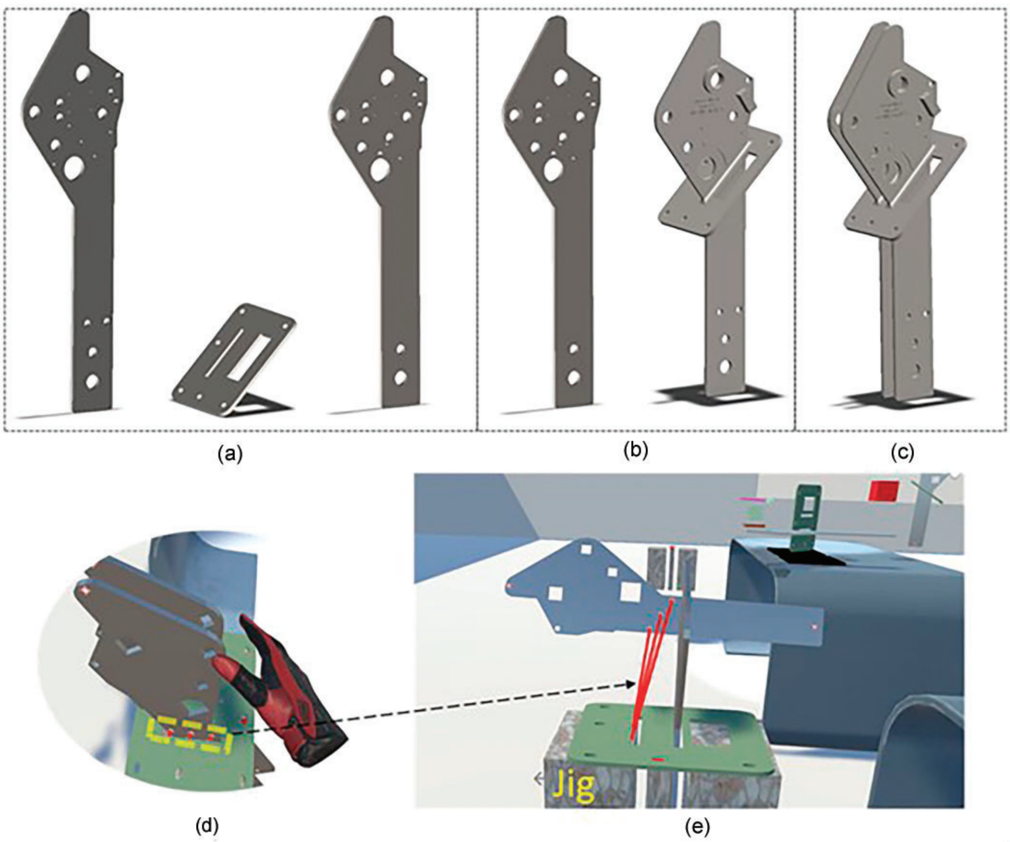


**Figure 8:** (a) Unconsolidated, (b) half-consolidated, and (c) consolidated hook assemblies. Unconsolidated and half-consolidated ones are assembled using jig in VR environment to control misalignment in 3D. (d) Edges of the assembly. (e) Exaggerated edges for visual illustration.

**Table 8:** Number of components used in this study (excluding auxiliary parts), connectors, and edges of the lifeboat hook assemblies.

| Hook alternatives | # of components | # of connectors | # of edges |
|---|---|---|---|
| Unconsolidated | 3 | 16 | 8 |
| Half-consolidated | 2 | 10 | 5 |
| Consolidated | 1 | 0 | 0 |

study, along with different versions of the PC-ed assemblies (Auyeskhan *et al.*, 2021). The hook assembly is an excellent example for demonstrating PC owing to its numerous parts.

Combinatorically, without any constraint, 30 hook assembly designs can be determined owing to the layout of the parts. For the details of how these assembly variants were obtained, readers can refer to Section S3 in the Supplementary file. Nevertheless, as it is impractical to include all of them, some constraints should be set. In the proposed approach, the DfAM-specific constraint is to maintain the build time and costs of all hook assembly alternatives the same. To do that, one must orient all the parts (excluding the auxiliary and miscellaneous components such as fasteners, nuts, and covers) to have a minimum support volume. However, the support volume of each design varies among assembly designs owing to the number of consolidated parts; hence it can be used within the intended design matrix.

After applying the constraints, only three assemblies are selected to demonstrate the importance of human aspects in the design, as shown in Fig. 8. These three assemblies vary in terms of the primary plates that constitute a substantial portion of support volume (Fig. 8a–c). The other parts are the same in all assemblies; thus, only these large plates will be used to evaluate nFRs. Table 8 shows brief information on the assemblies, such as the number of parts, connectors, and edges. Furthermore, Fig. 8d shows edges during the assembly process, while Fig. 8e shows the exaggerated one.

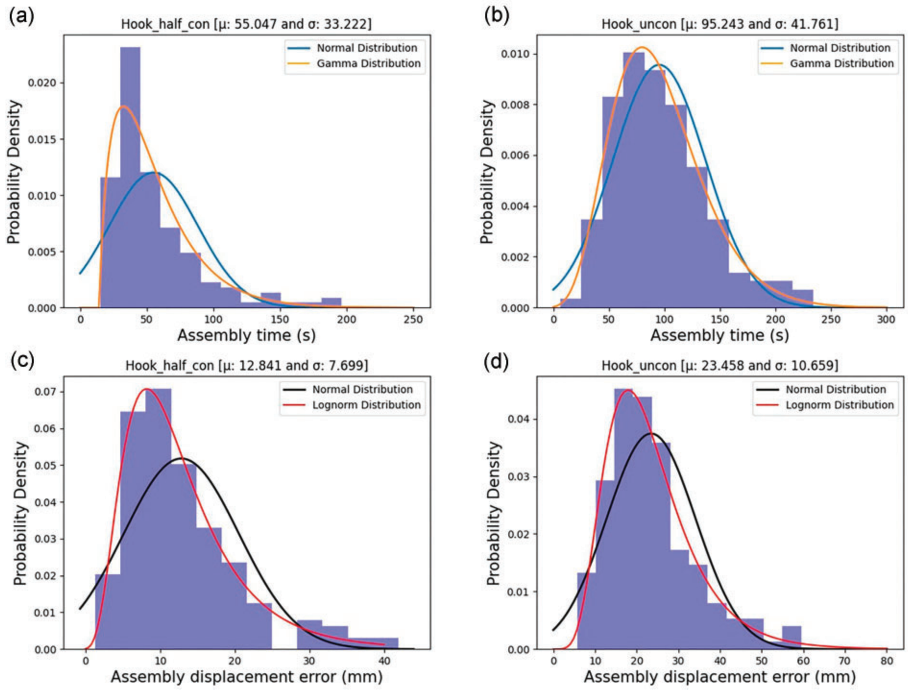


**Figure 9:** Representative fitted data of nFR1 and nFR2 with means ($\mu$) and standard deviations ($\sigma$) of half-consolidated hook designs [(a) and (c)] and unconsolidated hook designs [(b) and (d)].

**Table 9:** DRs of hook assembly.

| DRs | Less | Moderate | More |
|---|---|---|---|
| nFR1 (s) | 20 | 55.561 | 75 |
| nFR2 (mm) | 2 | 13.33 | 24 |
| nFR3 (mm$^3$) | 10 000–23 000 | 10 000–33 000 | 10 000–43 000 |

For nFR1 and nFR2, a true scale of the hook parts in VR is employed. Nevertheless, nFR3 possesses values of downscaled (by 1/3) alternatives, as one must fit the hook assembly within the L-PBF printer to demonstrate fabricability. Herein, fabricability by L-PBF of all the presented assembly designs is not included. Yet, the printability procedure of the consolidated hook assembly has been covered in Section S4 of the Supplementary file.

To re-emphasize, instead of CNs, MNs are considered because the original design and consolidated variations of hook assembly are already functionally valid. A reader can refer to a solved design matrix of FR–DP relation provided in Section S5 in the Supplementary file.

## 6. Results and Discussion

The experimental data were processed using an in-house python script before it could be evaluated using the framework. When AD-2 is involved, it is customary to use a normal distribution (Chen *et al.*, 2015), albeit this may not meet the demands of this study given that its values might reach negative infinity. The most appropriate distributions were selected and fitted for each system range of nFRs. For example, the system range of nFR1 can be interpreted as a gamma distribution as shown in Fig. 9a and b.

Normal distributions would not represent a real scenario as nFR1 > 0 and nFR2 > 0 because its random variables are the wait time until the $n^{\text{th}}$ assembly was assembled. Whereas lognormal distribution is ideal for nFR2 that cannot take negative values especially when a dataset is skewed to the right, hence it was chosen to be the best fitting distribution as it is seen from Fig. 9c and d.

Nevertheless, in terms of the means, for unconsolidated hook assembly, it took 73.0% more time to assemble (more nFR1), while the half-consolidated design has less 82.6% assembly displacement error (nFR2) than that of the unconsolidated one. This reveals the significance of PC in reducing the assembly time and assembly displacement error pertaining to the human aspect of design. However, it should be noted that to choose the best assembly design, in further steps the support volume (nFR3) will be also taken into account, which is compensated by the number of parts consolidated.

Furthermore, Table S6-1 contains the fitting parameters such as shape, location, scale, and mode of nFR1 and nFR2 for reference. The goodness of fit of the gamma and lognormal distributions can be confirmed using the Kolmogorov–Smirnov test (kstest). The kstest showed the data fit the distributions sufficiently (i.e., *P*-values > 0.05), as in Table S6-2.

Once the data processing is complete, a designer can select DRs that satisfy the desired nFRs (Suh, 2014). These DRs play a crucial role as they indicate the design's ability to accommodate variations in tolerance. The characteristic of AD theory, weighting factors are not needed as the tuning of the DRs already shows which nFR is more crucial (Suh, 1998). In this regard, the DRs are chosen in three distinct levels—less, moderate, and more. Each level expresses the importance of the specific nFR, and the selection of the levels facilitates the matching of the capabilities of a machine shop to manufacture a particular assembly design. For example, if a customer wants their product to be assembled quickly, he chooses nFR1 as less and looks for machine shops that could satisfy the customer's need on time.

**Table 10:** System ranges of nFR3 identified using Magics v24.1.

| nFR3_uniform | Unconsol | Half-consol | Consol |
|---|---|---|---|
| System ranges (mm$^3$) | 11 114.568–16 755.150 | 19 932.250–48 762.273 | 31 741.781–43 171.249 |

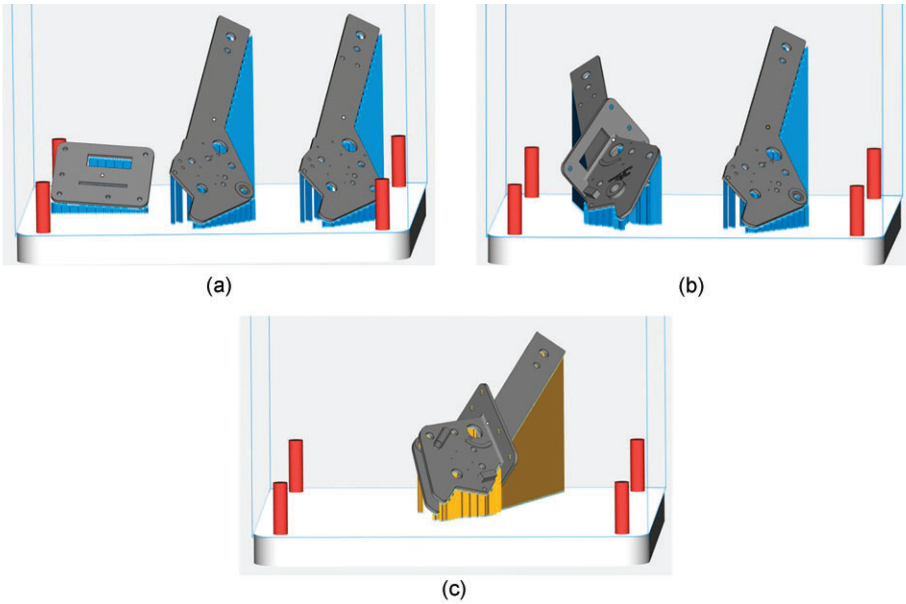


**Figure 10:** The support types of (a) unconsolidated, (b) half-consolidated, and (c) consolidated assemblies are default block, lines and point supports generated automatically.

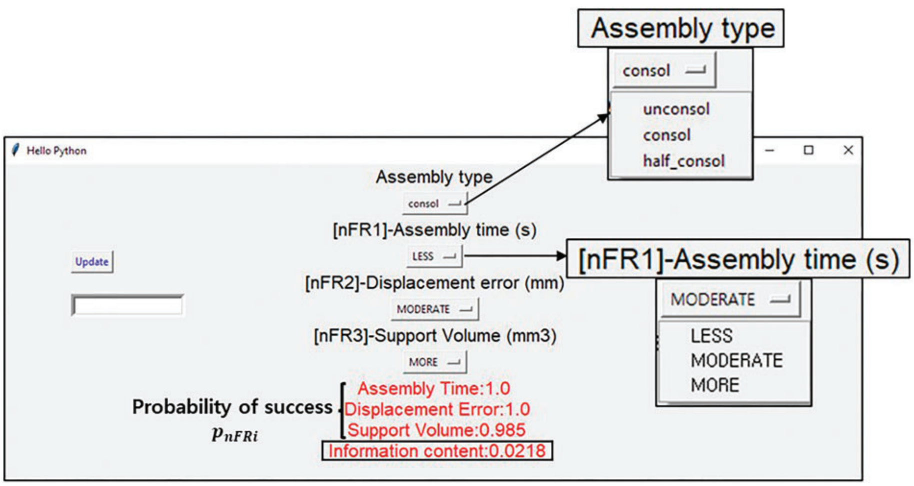


**Figure 11:** A capture of the in-house GUI to find the best assembly design based on AD-2. In this case, it is a consolidated type.

Table 9 shows the DRs of nFRs along with the corresponding levels. They are chosen based on the conducted experiments (i.e., nFR1 and nFR2) and characteristics of hook types (i.e., nFR3).

Therefore, herein, moderate DRs are set to be the means of the modes of gamma and lognormal distributions, for nFR1 and nFR2, respectively. The modes are used because they are defined as the values appearing most frequently in a dataset. Thus, moderate DR of nFR1 is 0–55.561 s while that of nFR2 is 0–13.33 mm. DRs of less and more are set to demonstrate quantification at lower and larger values, respectively, which can also be tuned by a user based on the experimental results.

Further, the system ranges of nFR1 and nFR2 can be found experimentally, but in the case of nFR3, the system ranges for each assembly are set to be between the minimum and maximum values of the support volume identified by Magics v.24.1, as shown in Table 10. nFR3 can be regarded to be uniformly distributed because the continuous uniform distribution exhibits the same probability of an outcome over a DR. The DRs of nFR3 were selected according to the values of assembly types. Figure 10 shows the support structures of three hook assemblies.

Calculating information content across the different DRs for various assemblies is a repetitive task and thus lends itself well

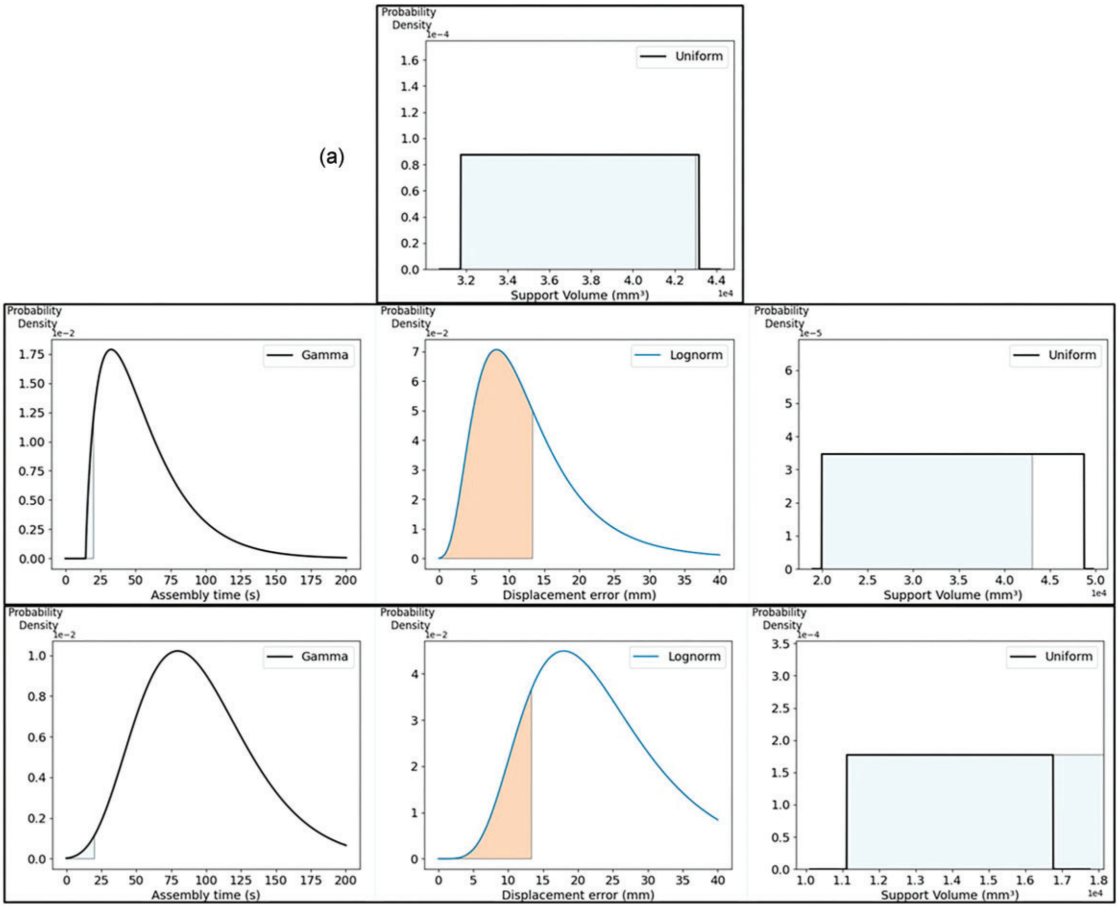


**Figure 12:** A part of GUI that displays probability densities of (a) consolidated, (b) half-consolidated, and (c) unconsolidated hook assembly designs.

**Table 11:** A representative case of computed $I_{\text{total}}$. Note that $p_{nFR1}$ and $p_{nFR2}$ stay constant in consolidated hook type as it does not involve assembling.

| | Unconsol | Half-consol | Consol |
|---|---|---|---|
| $p_{nFR1}$ | 0.0078 | 0.0409 | 1 |
| $p_{nFR2}$ | 0.15 | 0.6257 | 1 |
| $p_{nFR3}$ | 1.0 | 0.8001 | 0.985 |
| $I_{\text{total}}$ | 9.7312 | 5.6104 | 0.0218 |

to automation. For this reason, an in-house GUI for selecting the best assembly design has been developed. First, the assembly type should be chosen, following which corresponding nFRs with the desired level of DRs can be selected. Therefore, GUI calculates the probability densities of nFRs and the information content of that hook type, as shown in Fig. 11. At the same time, the probability densities of every hook type are plotted and calculated upon pressing "update" as shown in Fig. 12. Note that the GUI can be easily modified according to any assembly design; hence it is not limited to the hook assembly.

As a comparison, probability density plots and a summary of the table of information contents of each hook type are shown when DR{nFR1} = Less, DR{nFR2} = Moderate, and DR{nFR3} = More. Based on the information in AD-2, it can be concluded that the consolidated hook assembly is the best design in terms of information content, as demonstrated by the results in Table 11 and Fig. 12a, given the selected DRs. Additionally, Fig. 12b and c display the probability densities of half-consolidated and unconsolidated hook assemblies, respectively. Moreover, if one wants to utilize the framework for any other assemblies, one of the nFRs can be disabled. For example, for assemblies that require bolts, nuts, and riveting, nFR2 can be switched off, and the evaluation can be proceeded based on nFR1 and nFR3.

As can be observed, a new AD-based assembly-level DfAM framework enabled by VR led us to extract the human aspect of design, which has been presented for the first time to the best of the authors' knowledge. The applicability and versatility of both AD and VR ensure that human aspects can be numerically expressed, thus eliminating subjectivity in decision-making to a certain extent.

## 7. Conclusions and Future Works

This study presents a unique AM design decision framework incorporating DfA, DfAM, and AD theory to extract the most desirable assembly design in terms of probability density. The detailed workflow to improve assembly and AM productivities utilizing AD involves hitherto mostly disregarded human aspects of design at the early design stage. By assisting an assembly line worker with a VR environment in advance, nFRs can be quantified based on the interaction of human subjects with assembly design alternatives. The contribution of our proposed study is manifold and can be listed as follows:

(i) Provision of a structured and experimental base for verifying a design matrix for independence.
(ii) Quantification of nFR1 and nFR2 within VR scenes.
(iii) Demonstration of the framework on an industrial lifeboat hook assembly.
(iv) Extraction of the most preferred assembly based on specified DRs.
(v) Automation of a resultant workflow via a newly developed GUI.

As was shown, PC can produce several different assembly types. Our study can assist in determining the ideal assembly design to be printed using, e.g., L-PBF printers. However, the authors do not consider various build orientations; hence, the parts' costs are assumed to be constant. In future work, cost constraints can be lifted to involve multiple build orientations rather than just minimizing nFR3. Furthermore, the DRs when applying AD-2 must be experimentally identified, which might require extensive resources. However, once extracted, DRs will be applicable for multiple assembly designs at the detailed design stage. Moreover, this study shows that including human assembly processes in an AD-based AM decision framework can be potentially used before 3D printing any assembly designs.

## Credits to Authorship

U.A.: Conceptualization, methodology, software, investigation, validation, and writing – original draft.

C.A.S.: Methodology, software, validation, and writing – review & editing.

S.P.: Investigation, technical support, and management.

D.-H.K.: Conceptualization, methodology, and writing – review & editing.

I.D.J.: Conceptualization, methodology, and writing – review & editing.

N.K.: Conceptualization, methodology, funding acquisition, and writing – review & editing.

## Supplementary Data

Supplementary data is available at *JCDENG* Journal online.

## Acknowledgments

This work was supported by the Korea Institute of Energy Technology Evaluation and Planning (KETEP) grant funded by the Korea government (MOTIE, 20193310100030), and the Nuclear Safety Research Program through the Korea Foundation of Nuclear Safety (KoFONS) using the financial resource granted by the Nuclear Safety and Security Commission (NSSC) of the Republic of Korea. (No. 2003020).

## Conflict of interest statement

None declared.

## Data Availability

The raw/processed data to regenerate the findings cannot be shared owing to non-disclosure agreements. The source code for GUI is under a patent application stage and thus cannot be made publicly available currently.

## References

Abidi M. H., Al-Ahmari A., Ahmad A., Ameen W., & Alkhalefah H. (2019). Assessment of virtual reality-based manufacturing assembly training system. *International Journal of Advanced Manufacturing Technology*, **105**, 3743–3759. https://doi.org/10.1007/s00170-019-03801-3.

Agrawal R. (2022). Sustainable design guidelines for additive manufacturing applications. *Rapid Prototyping Journal*, **28**, 1221–1240. https://doi.org/10.1108/RPJ-09-2021-0251.

Asuero A. G., Sayago A., & González A. G. (2006). The correlation coefficient: An overview. *Critical Reviews in Analytical Chemistry*, **36**, 41–59. https://doi.org/10.1080/10408340500526766.

Auyeskhan U., Kim N., Kim C. S., Loi T. V., Choi J., & Kim D.-H. (2021). Design approach for additive manufacturing of a dynamically functioning system: Lifeboat hook. *International Journal of Precision Engineering and Manufacturing-Green Technology*, **9**, 1349–1367. https://doi.org/10.1007/s40684-021-00399-4.

Biswal R., Venkatesh V., & Arumaikkannu G. (2020). Investigation on part consolidation for additive manufacturing with SIMP method. *Materials Today: Proceedings*, **46**, 4954–4961. https://doi.org/10.1016/j.matpr.2020.10.381.

Boca M. A., Slatineanu L., & Sover A. (2021). Development of moulds for thermoforming using FFF additive manufacturing and axiomatic design. *IOP Conference Series: Materials Science and Engineering*, **1174**. https://doi.org/10.1088/1757-899x/1174/1/012016.

Boothroyd G., & Alting L. (1992). Design for assembly and disassembly. *CIRP Annals*, **41**, 625–636. https://doi.org/10.1016/S0007-8506(07)63249-1.

Boothroyd G., & Marinescu I. (2008). *Product design for manufacture and assembly*. Marcel Dekker, Inc.

Brookes J., Warburton M., Alghadier M., Mon-Williams M., & Mushtaq F. (2020). Studying human behavior with virtual reality: The Unity Experiment Framework. *Behavior Research Methods*, **52**, 455–463. https://doi.org/10.3758/s13428-019-01242-0.

Chayoukhi S., Bouaziz Z., & Zghal A. (2009). Costweld : A cost estimation system of welding based on the feature model. *Advances in Production Engineering & Management*, **4**, 263–274.

Chekurov S., Niklas K., Rossoni M., Redaelli D. F., & Colombo G. (2019). Axiomatic design to foster additive manufacturing-specific design knowledge. *ASME 2019 International Mechanical Engineering Congress and Exposition*, **14**, 1–9. https://doi.org/10.1115/IMECE2019-11480.

Chen D., Chu X., Sun X., Li Y., & Su Y. (2015). An information axiom based decision making approach under hybrid uncertain environments. *Information Science*, **312**, 25–39. https://doi.org/10.1016/j.ins.2015.03.054.

Delaš J., Škec S., & Štorga M. (2018). Application of axiomatic design principles in conceptual design. *MATEC Web of Conferences*, **223**. https://doi.org/10.1051/matecconf/201822301008.

Farid A. M., & Suh N. P. (2016). *Axiomatic design in large systems*. Springer International Publishing.

Gangwar M., Yadav Y. K., Gupta M., & Narain R. (2009). Axiomatic design: An aid in selecting right rapid prototyping process for new product development. *International Journal of Agile Manufacturing*, **11**, 45–56.

Green E., Estrada S., Gopalakrishnan P. K., Jahanbekam S., & Behdad S. (2022). A graph partitioning technique to optimize the physical integration of functional requirements for axiomatic design. *Journal of Mechanical Design*, **144**. https://doi.org/10.1115/1.4052702.

Harutunian V., Nordlund M., Tate D., & Suh N. P. (1996). Decision making and software tools for product development based on axiomatic design theory. *CIRP Annals*, **45**, 135–139. https://doi.org/10.1016/S0007-8506(07)63032-7.

Heikkilä L. J. (2020). Applications of axiomatic design in academic publications 2013-2018: A systematic literature review. Master's Thesis, University of VAASA.

Hines C. B. (2004). Time-of-day effects on human performance. *Journal of Catholic Education*, **7**, 390–413. https://doi.org/10.15365/joce.0703072013.

Jiang J., Xiong Y., Zhang Z., & Rosen D. W. (2022). Machine learning integrated design for additive manufacturing. *Journal of Intelligent Manufacturing*, **33**, 1073–1086. https://doi.org/10.1007/s10845-020-01715-6.

Kim S., & Moon S. K. (2020). A part consolidation design method for additive manufacturing based on product disassembly complexity. *Applied Sciences*, **10**. https://doi.org/10.3390/app10031100.

Kulak O., Cebi S., & Kahraman C. (2010). Applications of axiomatic design principles: A literature review. *Expert Systems with Applications*, **37**, 6705–6717. https://doi.org/10.1016/j.eswa.2010.03.061.

Lee D. G., & Suh N. P. (2006). Axiomatic design and fabrication of composite structures: Applications in robots, machine tools, and automobiles. *Industrial Robot*, **33**. https://doi.org/10.1108/ir.2006.04933bae.001.

Liu C., Le Roux L., Körner C., Tabaste O., Lacan F., & Bigot S. (2022). Digital twin-enabled collaborative data management for metal additive manufacturing systems. *Journal of Manufacturing Systems*, **62**, 857–874. https://doi.org/10.1016/j.jmsy.2020.05.010.

Mabrok M. A., Efatmaneshnik M., & Ryan M. J. (2015). Integrating nonfunctional requirements into axiomatic design methodology. *IEEE Systems Journal*, **11**, 2204–2214. https://doi.org/10.1109/jsyst.2015.2462073.

Maier J. R. A., & Fadel G. M. (2009). Affordance based design: A relational theory for design. *Research in Engineering Design*, **20**, 13–27. https://doi.org/10.1007/s00163-008-0060-3.

Mattsson S. (2013). What is perceived as complex in final assembly? To define, measure and manage production complexity. Thesis for the Degree of Licentiate of Engineering, Chalmers Reproservice.

Nie Z., Jung S., Kara L. B., & Whitefoot K. S. (2020). Optimization of part consolidation for minimum production costs and time using additive manufacturing. *Journal of Mechanical Design*, **142**. https://doi.org/10.1115/1.4045106.

Oh Y., & Behdad S. (2017). Assembly design framework for additive manufacturing (AM) based on axiomatic design (AD). In *Proceedings of the 67th Annual Conference and Expo of the Institute of Industrial Engineers 2017* (pp. 1024–1029).

Pradel P., Zhu Z., Bibb R., & Moultrie J. (2018). A framework for mapping design for additive manufacturing knowledge for industrial and product design. *Journal of Engineering Design*, **29**, 291–326. https://doi.org/10.1080/09544828.2018.1483011.

Rauch E., Matt D. T., & Dallasega P. (2016). Application of axiomatic design in manufacturing system design: A literature review. *Procedia CIRP*, **53**, 1–7. https://doi.org/10.1016/j.procir.2016.04.207.

Renjith S. C., Okudan Kremer G. E., & Park K. (2018). A design framework for additive manufacturing through the synergistic use of axiomatic design theory and TRIZ. In *Proceedings of the IISE Annual Conference and Expo 2018* (pp. 551–556).

Renjith S. C., Park K., & Okudan Kremer G. E. (2020). A design framework for additive manufacturing: Integration of additive manufacturing capabilities in the early design process. *International Journal of Precision Engineering and Manufacturing*, **21**, 329–345. https://doi.org/10.1007/s12541-019-00253-3.

Rodrigue H., & Rivette M. (2010). An assembly-level design for additive manufacturing methodology. https://doi.org/DOI:10.1007/978-2-8178-0169-8.

Salonitis K. (2016). Design for additive manufacturing based on the axiomatic design method. *International Journal of Advanced Manufacturing Technology*, **87**, 989–996. https://doi.org/10.1007/s00170-016-8540-5.

Schmelzle J., Kline E. V., Dickman C. J., Reutzel E. W., Jones G., & Simpson T. W. (2015). (Re)Designing for part consolidation: Understanding the challenges of metal additive manufacturing. *Journal of Mechanical Design*, **137**, 1–12. https://doi.org/10.1115/1.4031156.

Segovia M., & Garcia-Alfaro J. (2022). Design, modeling and implementation of digital twins. *Sensors*, **22**. https://doi.org/10.3390/s22145396.

Sossou G., Demoly F., Montavon G., & Gomes S. (2018). An additive manufacturing oriented design approach to mechanical assemblies. *Journal of Computational Design and Engineering*, **5**, 3–18. https://doi.org/10.1016/j.jcde.2017.11.005.

Sozo V., & Forcellini F. (2003). An axiomatic design software tool for decision making during the product conceptual design phase. *Product: Management & Development*, **2**, 41–52.

Suh N. P. (1995). Axiomatic design of mechanical systems. *Journal of Mechanical Design*, **117**, 2–10. https://doi.org/10.1115/1.2836467.

Suh N. P. (1998). Engineering design axiomatic design theory for systems. *Research in Engineering Design*, **10**, 189–209 https://doi.org/10.1007/s001639870001.

Suh N. P. (2001). *Axiomatic design: Advances and applications*. Oxford University Press.

Suh N. P. (2014). Designing-in of quality through axiomatic design. *IEEE Transactions on Reliability*, **44**, 256–264. https://doi.org/10.1109/24.387380.

Suh N. P., & Sekimoto S. (1990). Design of thinking design machine. *CIRP Annals*, **39**, 145–149. https://doi.org/10.1016/S0007-8506(07)61022-1.

Tamayo E. C., Khan Y. I., Qureshi A. J., & Al-Hussein M. (2019). Conceptual design of an automated steel wall framing assembly using axiomatic design and integrated function model. *Construction Robotics*, **3**, 83–101. https://doi.org/10.1007/s41693-019-00022-8.

Thompson M. K. (2013). Improving the requirements process in axiomatic design theory. *CIRP Annals*, **62**, 115–118. https://doi.org/10.1016/j.cirp.2013.03.114.

Thompson M. K., & Mischkot M. (2015). Design of test parts to characterize micro additive manufacturing processes. *Procedia CIRP*, **34**, 223–228. https://doi.org/10.1016/j.procir.2015.07.065.

Toguem S.-C. T., Mehdi-Souzani C., Nouira H., & Anwer N. (2020). Axiomatic Design of Customised Additive Manufacturing Artefacts. *Procedia CIRP*, **91**, 899–904. https://www.sciencedirect.com/science/article/pii/S2212827120309203.

Wang H., Li H., Tang C., Zhang X., & Wen X. (2020). Unified design approach for systems engineering by integrating model-based systems. *Systems Engineering*, **23**, 49–64. https://doi.org/10.1002/sys.21505.

Weber J., Kößler J., & Paetzold K. (2015). An approach for industrial application of axiomatic design. In *Proceedings of the 20th International Conference on Engineering Design (ICED15)* (Vol. **2**, pp. 1–10).

Wright T. P. (1936). Factors affecting the cost of airplanes. *Journal of the Aeronautical Sciences*, **3**, 122–128. https://doi.org/10.2514/8.155.

Yang S., Santoro F., Sulthan M. A., & Zhao Y. F. (2019). A numerical-based part consolidation candidate detection approach with modularization considerations. *Research in Engineering Design*, **30**, 63–83. https://doi.org/10.1007/s00163-018-0298-3.

Yang S., Santoro F., & Zhao Y. F. (2018). Towards a numerical approach of finding candidates for additive manufacturing-enabled part consolidation. *Journal of Mechanical Design*, **140**. https://doi.org/10.1115/1.4038923.

Yang S., & Zhao Y. F. (2016). Conceptual design for assembly in the context of additive manufacturing. In *Solid Freeform Fabrication 2016: Proceedings of the 27th Annual International Solid Freeform Fabrication Symposium – An Additive Manufacturing Conference (SFF 2016)* (pp. 1932–1944).

Zhang R., Cha J., & Lu Y. (2007). A conceptual design model using axiomatic design, functional basis and TRIZ. In *Proceedings of the 2007 IEEE International Conference on Industrial Engineering and Engineering Management* (pp. 1807–1810). IEEE International Conference on IEEM. https://doi.org/10.1109/IEEM.2007.4419504.



**Received:** December 24, 2022. **Revised:** April 25, 2023. **Accepted:** April 26, 2023